Advanced Image Reconstruction Methods for Photoacoustic Tomography

Mark A. Anastasio, Kun Wang, and Robert Schoonover

Department of Biomedical Engineering

Washington University in St. Louis

Washington University in St. Louis
School of Engineering & Applied Science

Outline

- Photoacoustic/thermoacoustic tomography
  - Very brief review
- Issues for image reconstruction
  - Incorporation of transducer effects into imaging model
  - Incomplete data image reconstruction
  - Non-uniform acoustic properties of object (layered media)

Washington University in St.Louis
School of Engineering & Applied Science

Schematic of PAT

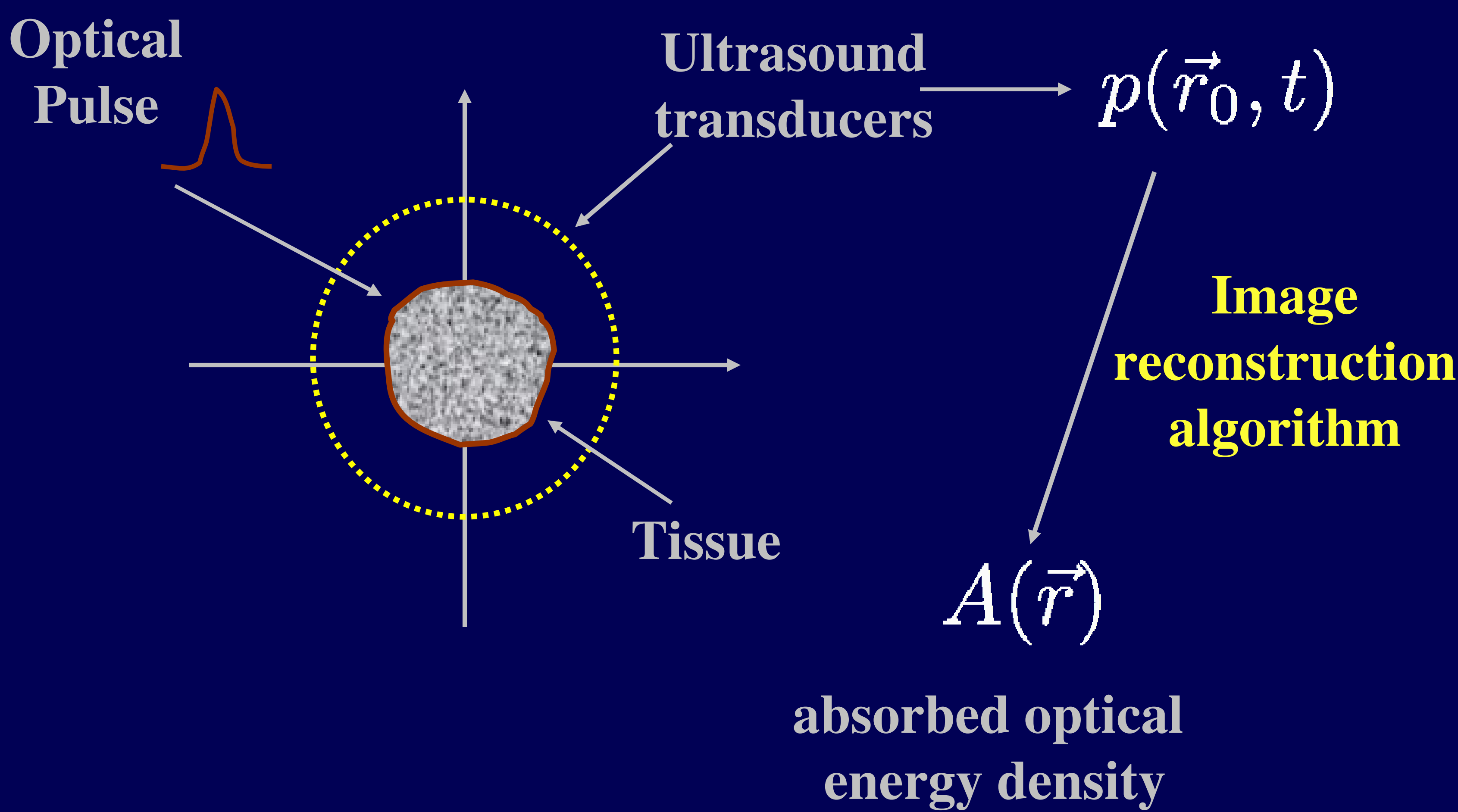

Washington University in St. Louis
School of Engineering & Applied Science

Conventional PAT imaging model

- **Conventional imaging model (assuming point-like transducers)**

$$p(\mathbf{r}_0, t) = \frac{\beta}{4\pi C_p} \int_V d^3\mathbf{r}' A(\mathbf{r}') \, \frac{d}{dt'} \frac{\delta(t')}{|\mathbf{r}_0 - \mathbf{r}'|}\Bigg|_{t' = t - \frac{|\mathbf{r} - \mathbf{r}_0|}{c}}$$

OR

$$g(\mathbf{r}_0, \bar{t} = ct) = \int_V d^3\mathbf{r} A(\vec{r}) \delta(\bar{t} - |\mathbf{r} - \mathbf{r}_0|)$$

where

$$g(\mathbf{r}_0, \bar{t} = ct) = \frac{4\pi C_p t}{\beta} \int_0^t dt' p(\mathbf{r}_0, t')$$

Issue #1 for image reconstruction: <u>Ultrasound transducer model</u>

- Conventional PAT reconstruction algorithms assume the ultrasound transducer is "point-like".
- In reality, the finite area of the transducer surface will result in an anisotropic detector response.
- Moreover, the measured pressure signal is degraded by the acousto-electrical response of the transducer.
- We have developed a methodology for including the transducer response in the PAT imaging model

An Example of the Degradation Caused by Finite Aperture Size of Transducer

- **Phantom**: uniform spheres extending from the center to 10mm
- **Transducers**: planar transducer of dimension $4*4mm^2$ on a sphere of radius 25mm
- **Forward model**: spherical Radon transform (SRT) averaged over the transducer surface
- **Reconstruction algorithm**: filtered back projection (FBP)

D. Finch et al., SIAM J Math Anal, 2007

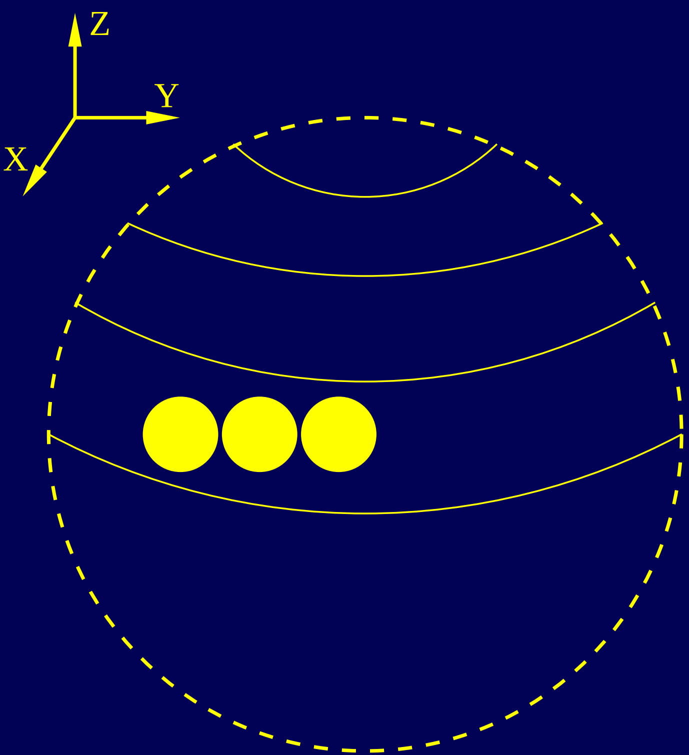

Ignoring Transducer Size Reconstruction Results

- **Blurring effect is more significant for**
  - objects further away from the center
  - tangent direction

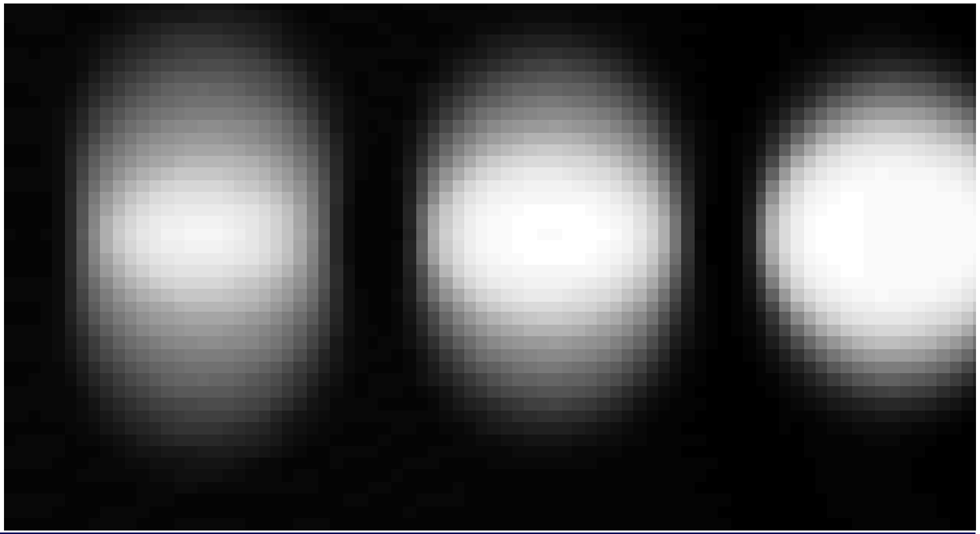

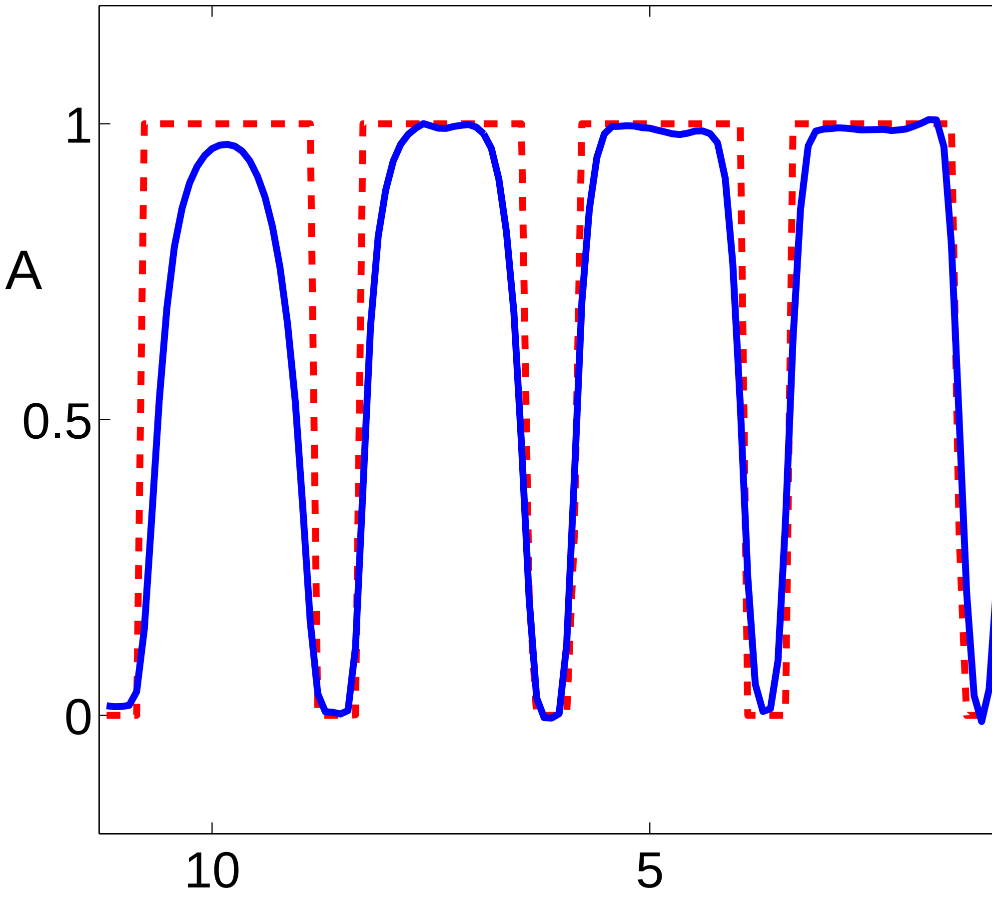

Washington University in St. Louis
School of Engineering & Applied Science

Discretization of imaging model

- **Operator form of continuous-to-continuous (C-C) mapping:**

$$p(\mathbf{r}_0, t) = H_{cc}A(\mathbf{r})$$

- **Digital imaging systems are described by continuous-to-discrete (C-D) mappings:**

$$\mathbf{p} = D_{\sigma\tau}H_{cc}A(\mathbf{r}) = H_{cd}A(\mathbf{r})$$

vector of pressure measurements

discretization operator

Discretization of imaging model

- **The discretization operator is defined as:**

$$p_{[mS+s]} = \left[\mathcal{D}^{(p)}_{\sigma\tau} p(\mathbf{r}_0, t)\right]_{[mS+s]} \equiv \int_{-\infty}^{\infty} dt\; \tau_s(t) \int_{\Omega_0} d\Omega_0\; p(\mathbf{r}_0, t)\sigma_m(\mathbf{r}_0)$$

m : transducer location index

s : time sample index

sampling apertures

- **Ideal case (Dirac delta sampling):**

$$p_{[mS+s]} = p(\mathbf{r}_{0,m}, s\Delta T)$$

Washington University in St. Louis
School of Engineering & Applied Science

Discrete-to-discrete (D-D) imaging model

- To perform iterative image reconstruction, a D-D imaging model is required.
- Obtained by substitution of a finite-dimensional object representation into the C-D imaging model.
- Object representation: $$A_a(\mathbf{r}) = \sum_{n=1}^{N} \theta_{[n]} \phi_n(\mathbf{r})$$

spherical expansion functions

- D-D imaging model:

$$\mathbf{p}_a = \mathcal{H}_{CD}\mathbf{A}_a(\mathbf{r}) = \sum_{n=1}^{N} \theta_{[n]} \mathcal{H}_{CD}\{\phi_n(\mathbf{r})\} \equiv \mathbf{H}\boldsymbol{\theta}$$

system matrix

K. Wang, et al, An Imaging Model Incorporating Ultrasonic Transducer Properties for Three-Dimensional Optoacoustic Tomography, IEEE TMI, 30, 2011.

Washington University in St. Louis
School of Engineering & Applied Science

Discrete-To-Discrete Imaging System

- **Explicit form of system matrix:**

$$[\mathbf{H}]_{qS+s,n} = h^e(t) * h_n^s(\mathbf{r}_{0,q}, t) * p_n(\mathbf{r}_{0,q}, t)\Big|_{t=s\Delta T}$$

electrical impulse response (measured)

Washington University in St. Louis
School of Engineering & Applied Science

Discrete-To-Discrete Imaging System

- **Explicit form of system matrix:**

$$[\mathbf{H}]_{qS+s,n} = h^e(t) * h_n^s(\mathbf{r}_{0,q}, t) * p_n(\mathbf{r}_{0,q}, t)\Big|_{t=s\Delta T}$$

spatial impulse response

$$h_a^s(\mathbf{r}_{0,q}, \mathbf{r}, t) = \sum_{n=0}^{N-1} h_n^s(\mathbf{r}_{0,q}, t)\phi_n(\mathbf{r}),$$

Washington University in St. Louis
School of Engineering & Applied Science

Discrete-To-Discrete Imaging System

- **Explicit form of system matrix:**

$$\left[\mathbf{H}\right]_{qS+s,n} = h^e(t) * h_n^s(\mathbf{r}_{0,q},t) * p_n(\mathbf{r}_{0,q},t)\Big|_{t=s\Delta T}$$

$$p_n(\mathbf{r}_{0,q},t) = \frac{\beta}{4\pi C_p}\int_V d^3\mathbf{r}\;\phi_n(\mathbf{r})\frac{d}{dt}\frac{\delta(t-\frac{|\mathbf{r}_{0,q}-\mathbf{r}|}{c_0})}{|\mathbf{r}_{0,q}-\mathbf{r}|}$$

$$\equiv \begin{cases} \frac{\beta c_0^2}{2C_pR_{q,n}}(R_{q,n}-c_0t), & \text{for } \frac{R_{q,n}-\epsilon}{c_0}\le t<\frac{R_{q,n}+\epsilon}{c_0} \\ 0, & \text{otherwise} \end{cases},$$

pressure produced by spherical voxel

Washington University in St. Louis
School of Engineering & Applied Science

Computer-Simulation Studies for Noiseless Data

- **Phantom**: thin section of depth 0.07mm consisting cylindrical structures
- **Transducers**: planar transducers of size 4*4mm^2 on single ring of radius 25mm lying in the central plane of the phantom (x-o-y plane).
- **Simulation data**: of higher resolution (1024*1024*2)
- **Reconstruction**: of lower resolution (512*512*1).

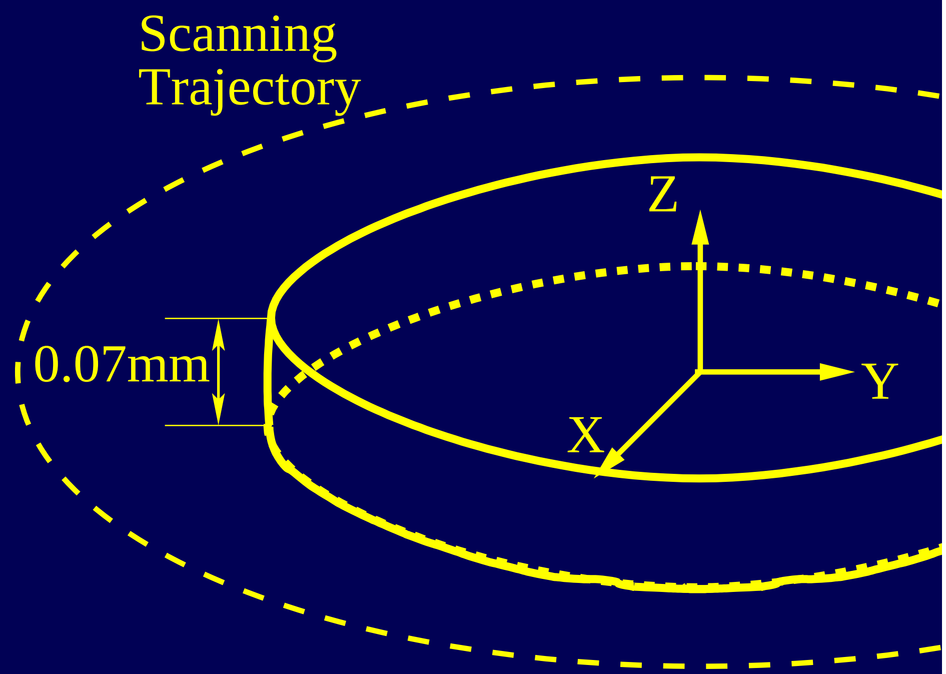

Washington University in St. Louis
School of Engineering & Applied Science

Compensation Model Gives Almost ‘Perfect’ Results for Noiseless Data

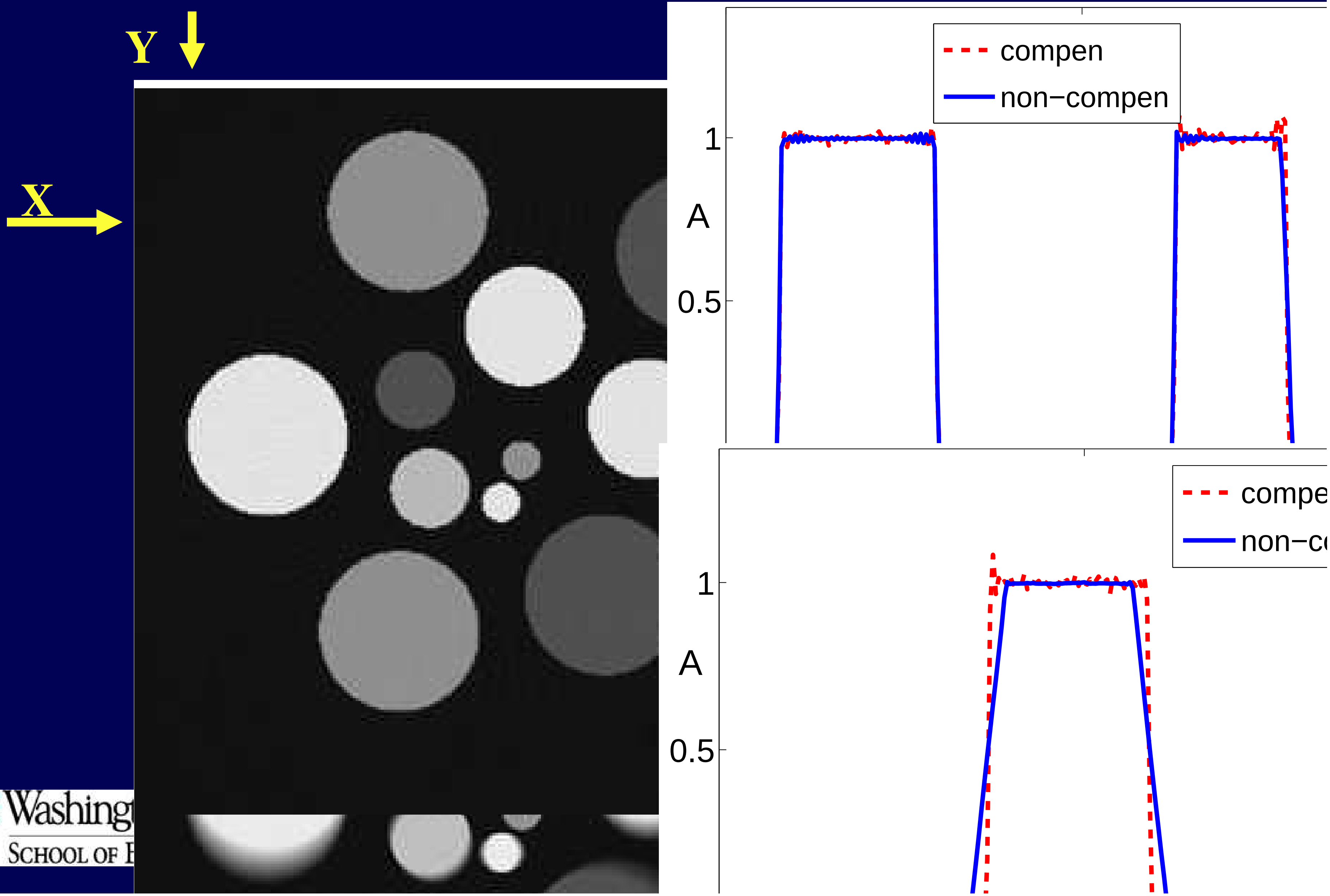

Resolution-Standard Deviation Curves

- **Use of the proposed imaging model can enhance spatial resolution in the reconstructed images.**

- **As expect, this comes at the cost of increased noise levels.**

- **This reflects that the solution to the inverse problem becomes less stable.**

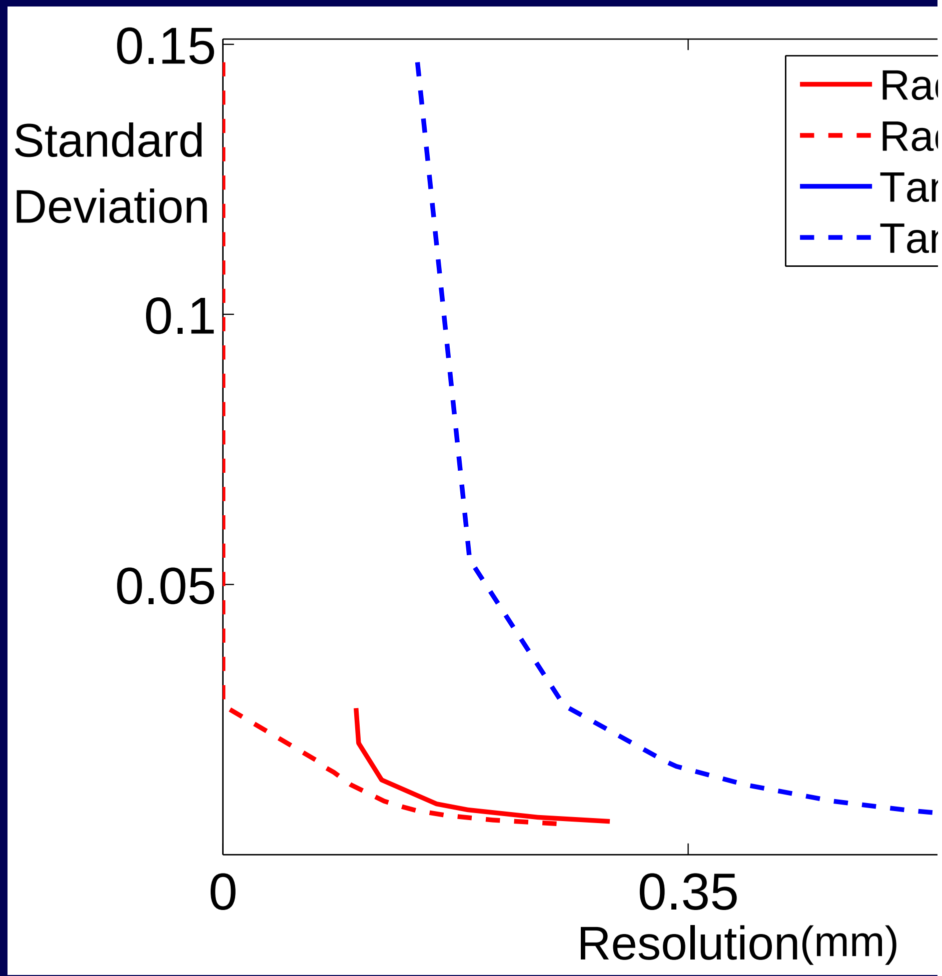

Washington University in St. Louis
SCHOOL OF ENGINEERING & APPLIED SCIENCE

Experimental Evaluations (geometry)

- **Phantom**: crossing hairs with the bottom half illuminated (from center to ~40mm)
- **Transducers**: arc scan array with radius 65mm consisting of 64 transducers of size 2*2 mm^2
- **Reconstruction**: by compensation and non-compensation models

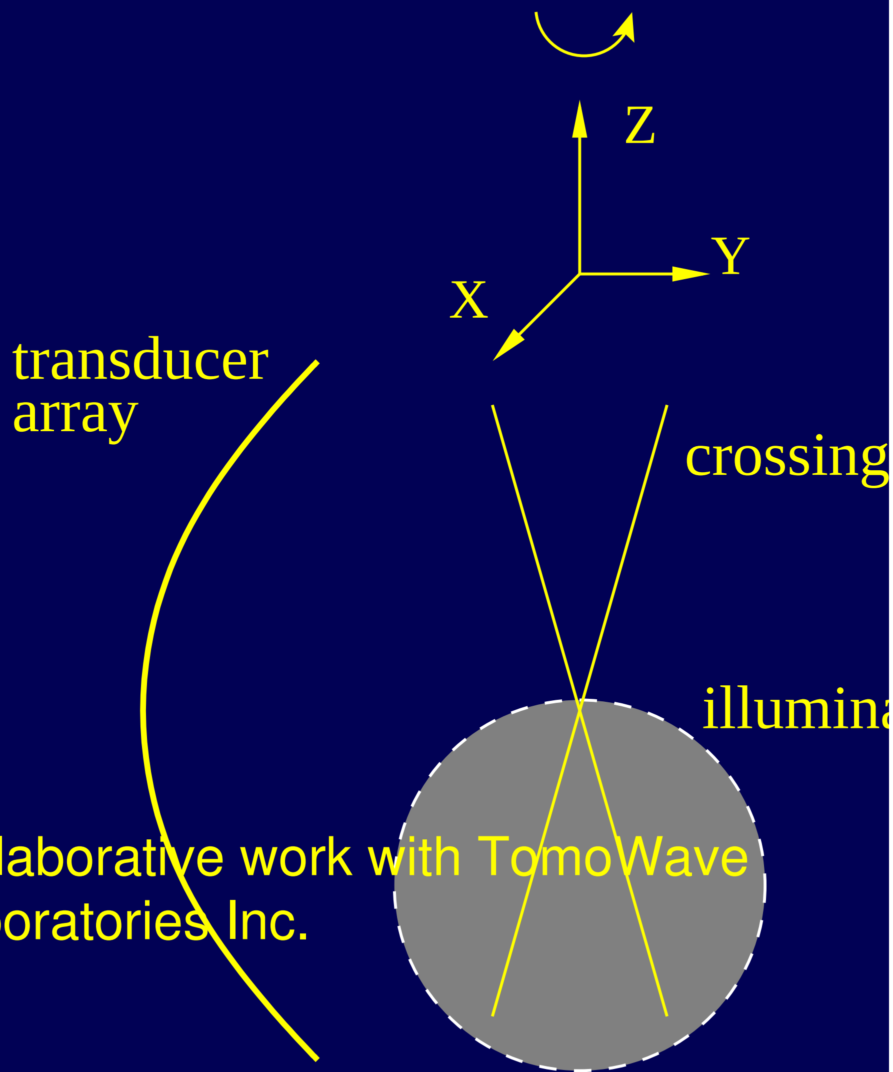

Collaborative work with TomoWave Laboratories Inc.

Washington University in St. Louis
School of Engineering & Applied Science

Experimental results

standard imaging model

new imaging model

Issue #2 for image reconstruction: Incomplete data

- For “exact” 3D image reconstruction using analytic reconstruction methods, pressure measurements must be acquired on a 2D surface that encloses the object.

- There remains an important need for robust reconstruction algorithms that work with limited data sets.

- We are developing/applying iterative image reconstruction methods for 3D PAT.

Example of real-data study: 3D Mouse Scanner

- Arc-shaped transducer array with 64 elements
- The mouse was rotated about z-axis over 2π
- ‘Full-data’: 180 view angles
- ‘Half-data’: 90 view angles
- Reconstruction algorithms
  - FBP algorithm
  - PLS algorithm

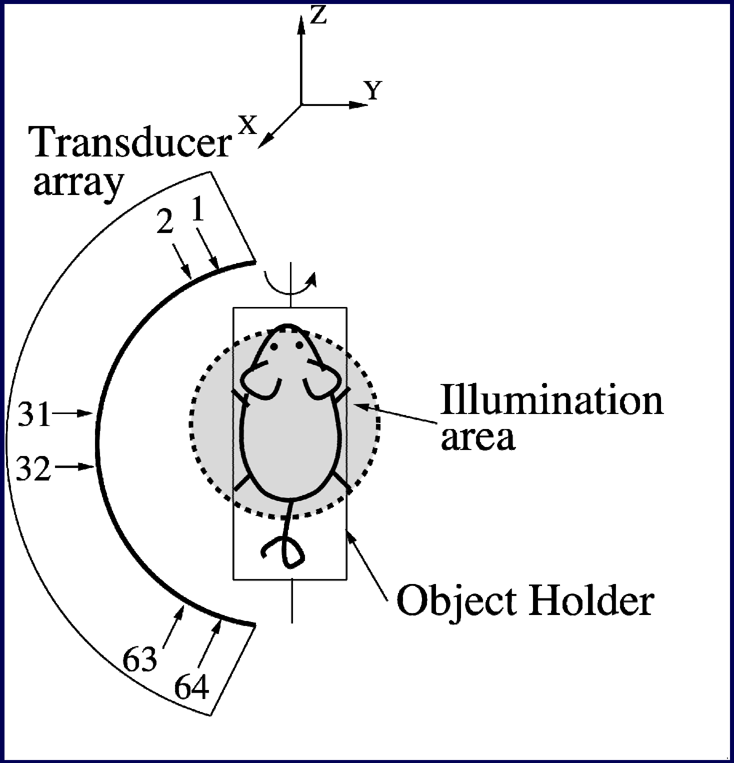

Collaborative work with TomoWave Laboratories Inc.

3D Rendering of Reconstructed Images

FBP using ‘full-data’

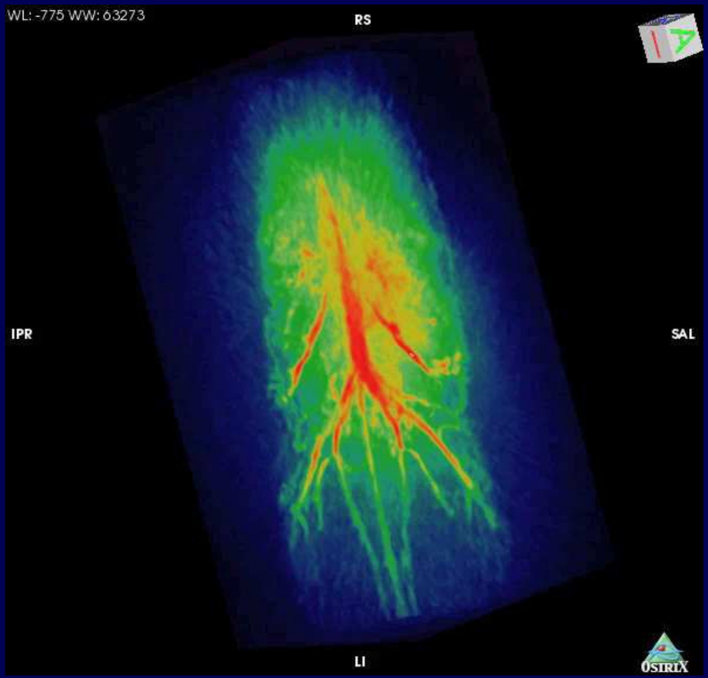

PLS using ‘half-data’

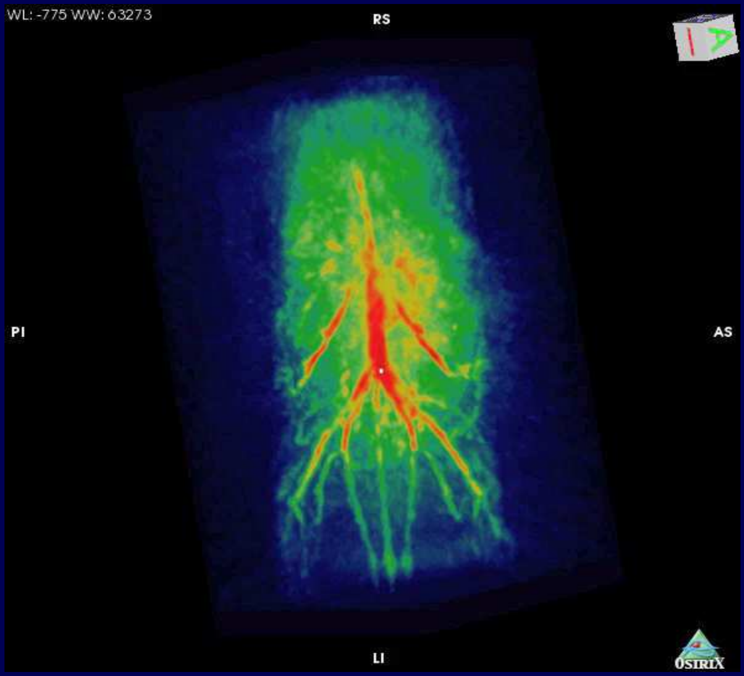

Washington University in St. Louis
SCHOOL OF ENGINEERING & APPLIED SCIENCE

2D Slices across Blood Vessels

FBP from 'full-data'

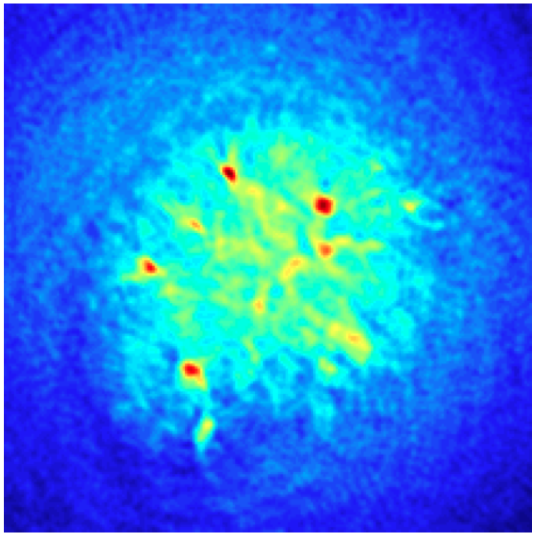

FBP from 'half-data'

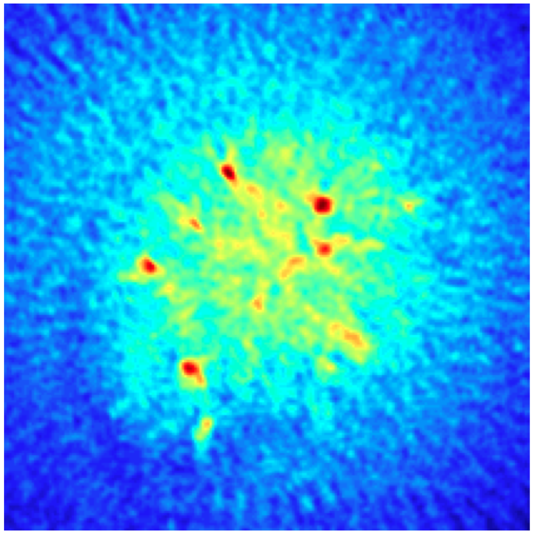

PLS from 'half-data'

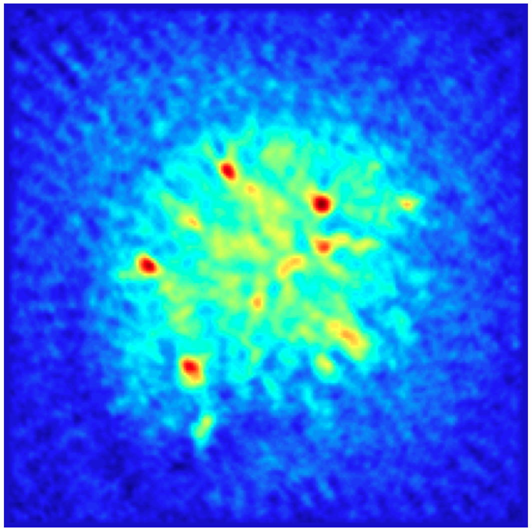

Washington University in St. Louis
SCHOOL OF ENGINEERING & APPLIED SCIENCE

Compressive sensing-inspired approaches

- Optimization problem:

$$\hat{\theta} = \arg\min_{\theta} \|\theta\|_{\mathrm{TV}}$$
$$\text{s.t.} \quad |\mathbf{p} - \mathbf{H}\,\theta| \leq \varepsilon$$
$$\theta \geq \mathbf{0}$$

- We implemented the ASD-POCS to solve the optimization problem. (Sidky and Pan, *Phys. Med. Biol.*, 7, 2008)

Collaborative work with Drs. E. Sidky and X. Pan (UChicago)

Computer-simulations

- **Scanning radius: 65mm**
- **Sampling rate: 20MHz**

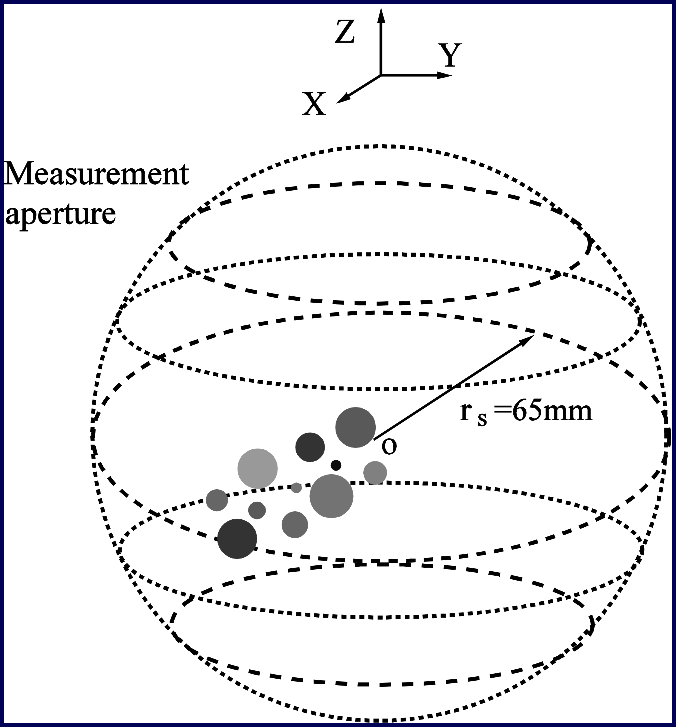

Transducers on a sphere

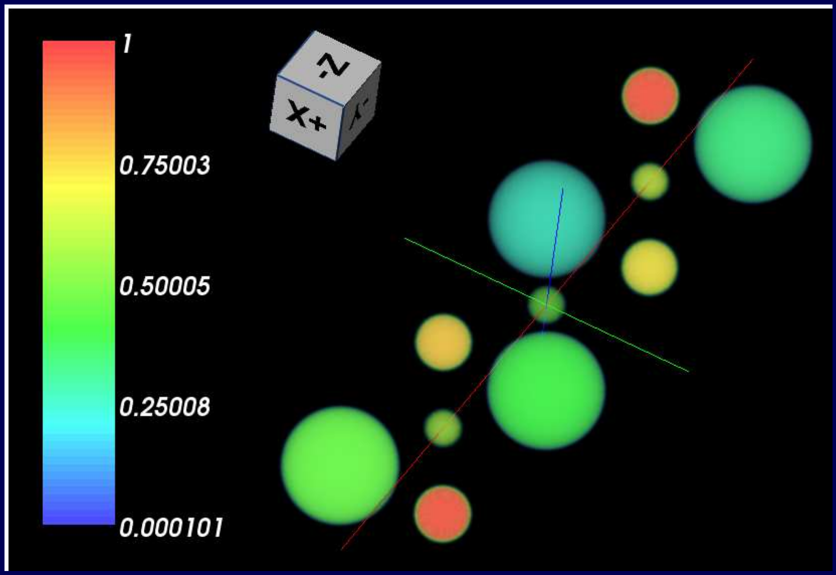

3D phantom

FBP Requires Data to be Densely Sampled over Space

- **'Full-data': 128*360 transducers**
- **'Limited-data': 8*15 transducers**

Full-data

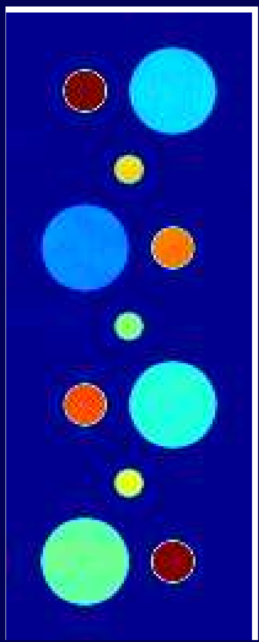

Limited-data

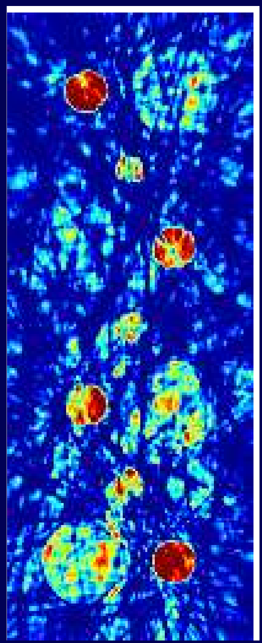

Image profiles

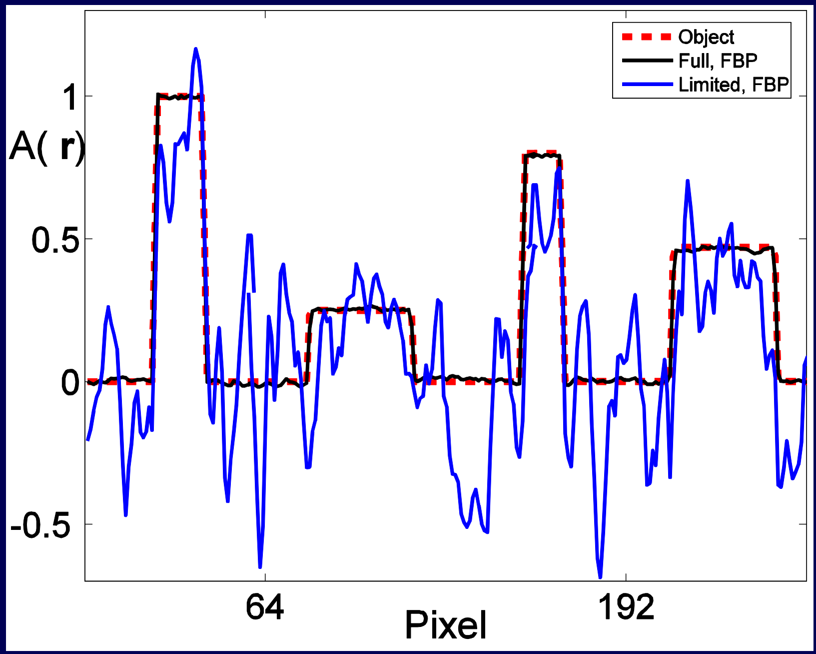

TV Algorithm Outperforms Conventional Algorithms (noisy)

- **Reconstructed images from limited-data contaminated by 0.5% Gaussian noise.**

ART

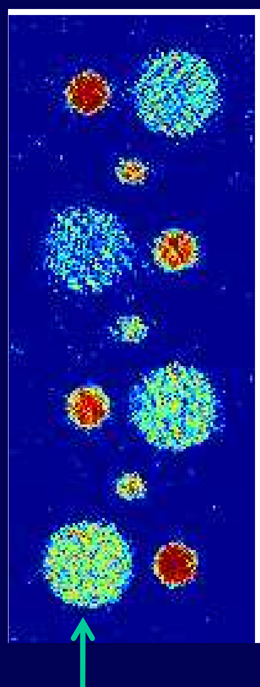

TV

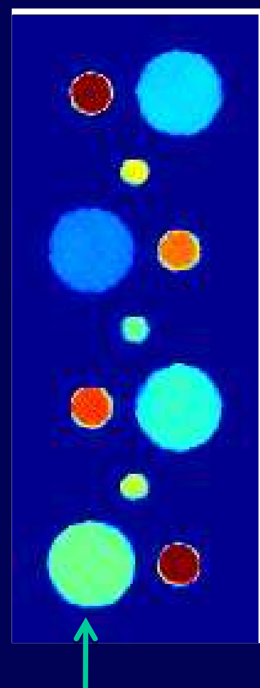

Image profiles

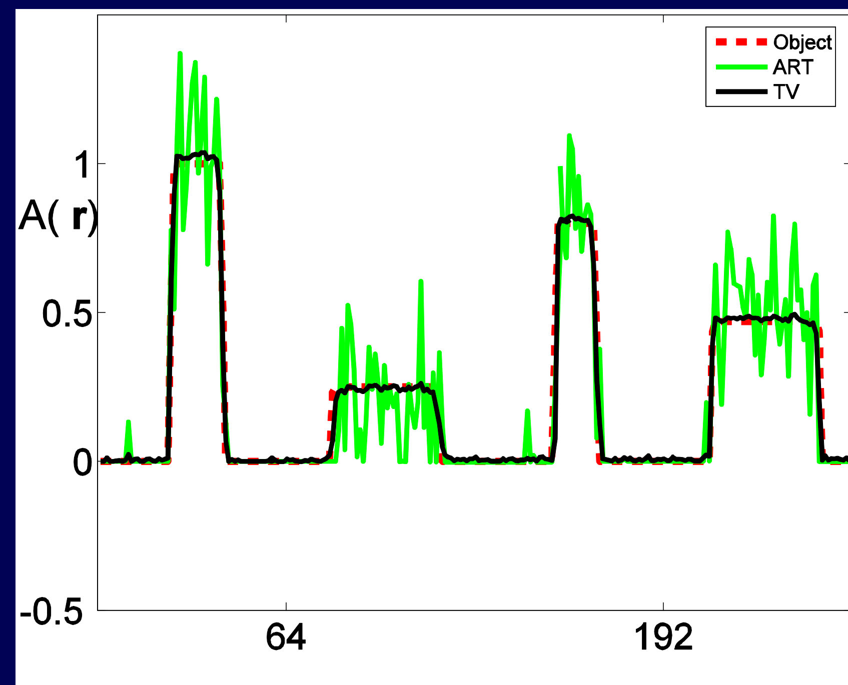

Washington University in St.Louis
School of Engineering & Applied Science

Issue #3 for image reconstruction: Acoustic inhomogeneities

- **Conventional PAT reconstruction algorithms assume the object of interest is acoustically homogeneous.**
- **In medical imaging applications this assumption is often not warranted.**
- **We have developed an analytic reconstruction formula for use with layered acoustic media**

R.W. Schoonover and M.A. Anastasio, "Image reconstruction in photoacoustic tomography involving layered acoustic media," ***J. Opt. Soc. Am. A*** **28, 1114–1120 (2011).**

Washington University in St.Louis
School of Engineering & Applied Science

Generic Layered Medium

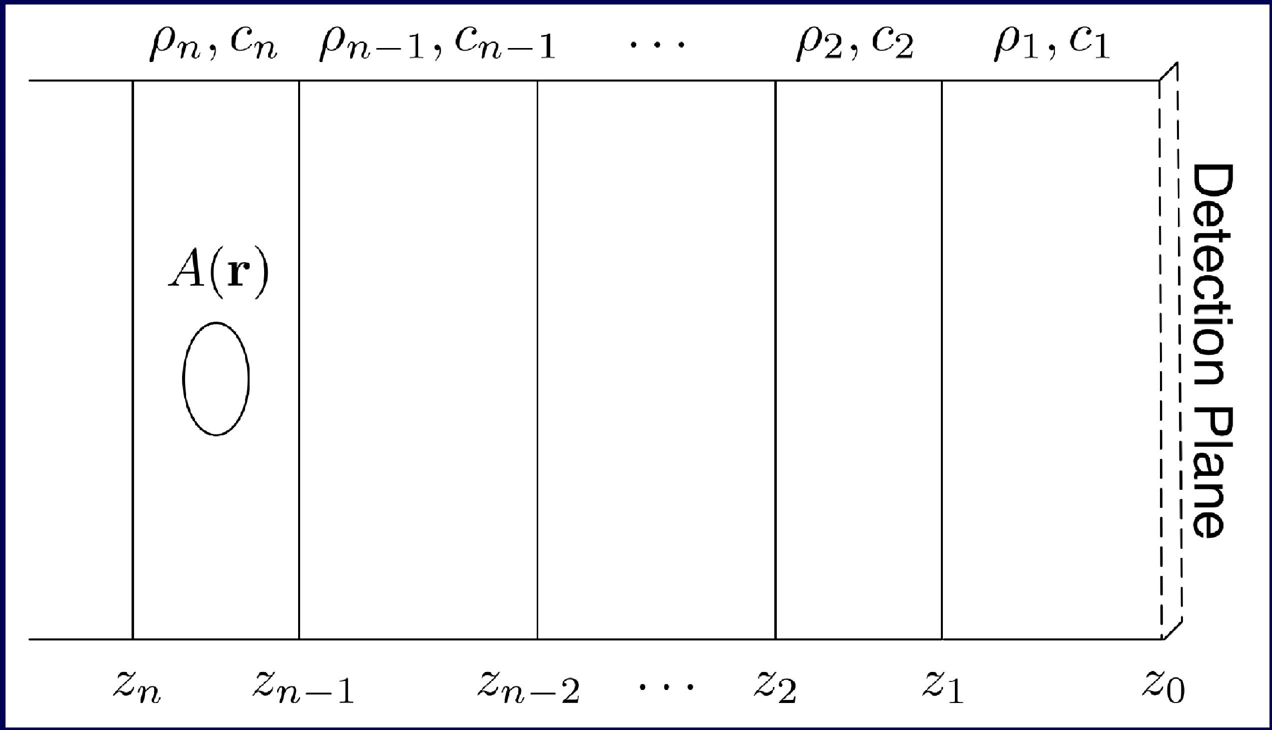

$$\rho(\mathbf{r}) = \rho_m \quad \text{for} \quad z_m \leq z < z_{m-1}$$

$$c(\mathbf{r}) = c_m \quad \text{for} \quad z_m \leq z < z_{m-1}$$

Washington University in St. Louis
School of Engineering & Applied Science

Imaging Model for Layered Medium

Develop a Green function for layered medium through use of Angular Spectrum decomposition:

$$G_P^{meas}(\mathbf{r}, \mathbf{r}'; \omega) = \iint_\infty \frac{\mathrm{d}^2 k_\parallel}{(2\pi)^2} e^{i\mathbf{k}_\parallel \cdot \mathbf{r}} a_1(\mathbf{k}_\parallel; \mathbf{r}')$$

determined from B.C.s

Imaging model:

$$p(\mathbf{r}, \omega) = \frac{i\omega\beta H(\omega)}{C_P} \iiint_V \mathrm{d}^3 r' \, G_P^{meas}(\mathbf{r}, \mathbf{r}'; \omega) A(\mathbf{r}')$$

Washington University in St.Louis
School of Engineering & Applied Science

Acoustic boundary conditions

B.C.s enforced at each layer

$$\tilde{p}(\mathbf{r},\omega)\big|_{z_m^-} = \tilde{p}(\mathbf{r},\omega)\big|_{z_m^+} \quad \forall m,$$

$$\frac{1}{\rho_{m+1}}\frac{\partial \tilde{p}}{\partial z}\bigg|_{z_m^-} = \frac{1}{\rho_m}\frac{\partial \tilde{p}}{\partial z}\bigg|_{z_m^+} \quad \forall m$$

A linear system of equations can be established to determine Green function.

- Algebraic solution

Solution: Three-Layered Medium

For a three layer medium with the object located in the layer furthest from the detection plane:

$$\mathcal{A}(\mathbf{k}_{\|}; k_z^{(m)}) = \frac{C_P k_z^{(m)}}{i\omega\beta H(\omega)} \frac{1 + e^{2ik_z^{(f)}d_f} r_{mf}(\mathbf{k}_{\|},\omega) r_{fs}(\mathbf{k}_{\|},\omega)}{e^{ik_z^{(s)}d} e^{ik_z^{(f)}d_f} t_{mf}(\mathbf{k}_{\|},\omega) t_{fs}(\mathbf{k}_{\|},\omega)} \tilde{p}(\mathbf{k}_{\|},\omega)$$

The label *m* refers to the first layer (muscle), the label *f* refers to the second layer (fat) and the label *s* refers to the third layer (skin).

The thicknesses of the layers are d_f (fat layer) and d_s (skin layer).

Washington University in St. Louis
School of Engineering & Applied Science

Image Reconstruction Model for Three-Layered Medium

Reflection and transmission coefficients:

$$r_{ij}(\mathbf{k}_{\|},\omega) = \frac{\eta_i k_z^{(j)}(\mathbf{k}_{\|},\omega) - \eta_j k_z^{(i)}(\mathbf{k}_{\|},\omega)}{\eta_i k_z^{(j)}(\mathbf{k}_{\|},\omega) + \eta_j k_z^{(i)}(\mathbf{k}_{\|},\omega)}$$

$$t_{ij}(\mathbf{k}_{\|},\omega) = \frac{2\eta_i k_z^{(j)}(\mathbf{k}_{\|},\omega)}{\eta_i k_z^{(j)}(\mathbf{k}_{\|},\omega) + \eta_j k_z^{(i)}(\mathbf{k}_{\|},\omega)}$$

Images reconstructed from noiseless data

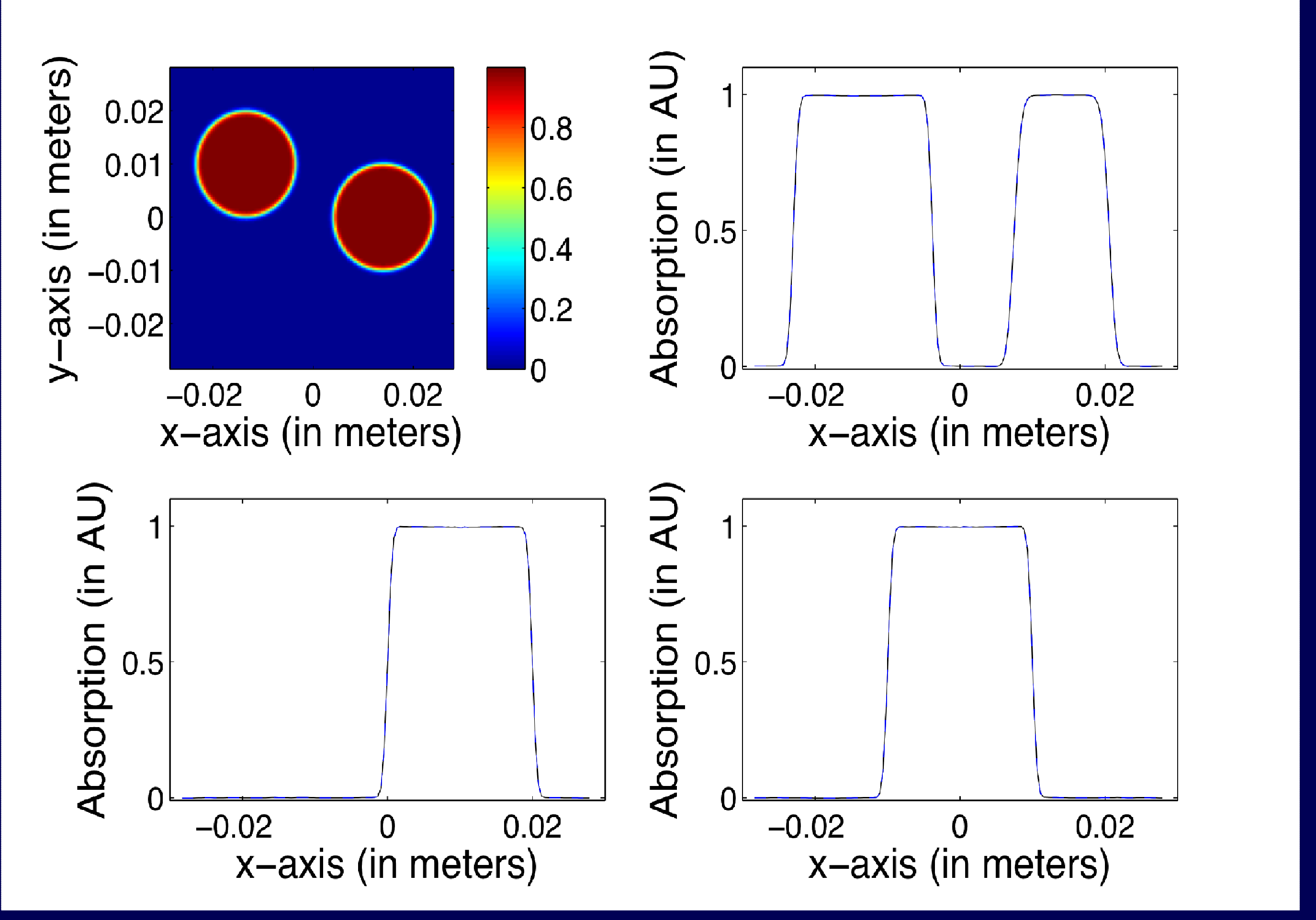

Washington University in St. Louis
School of Engineering & Applied Science

Images reconstructed assuming a homogenous medium

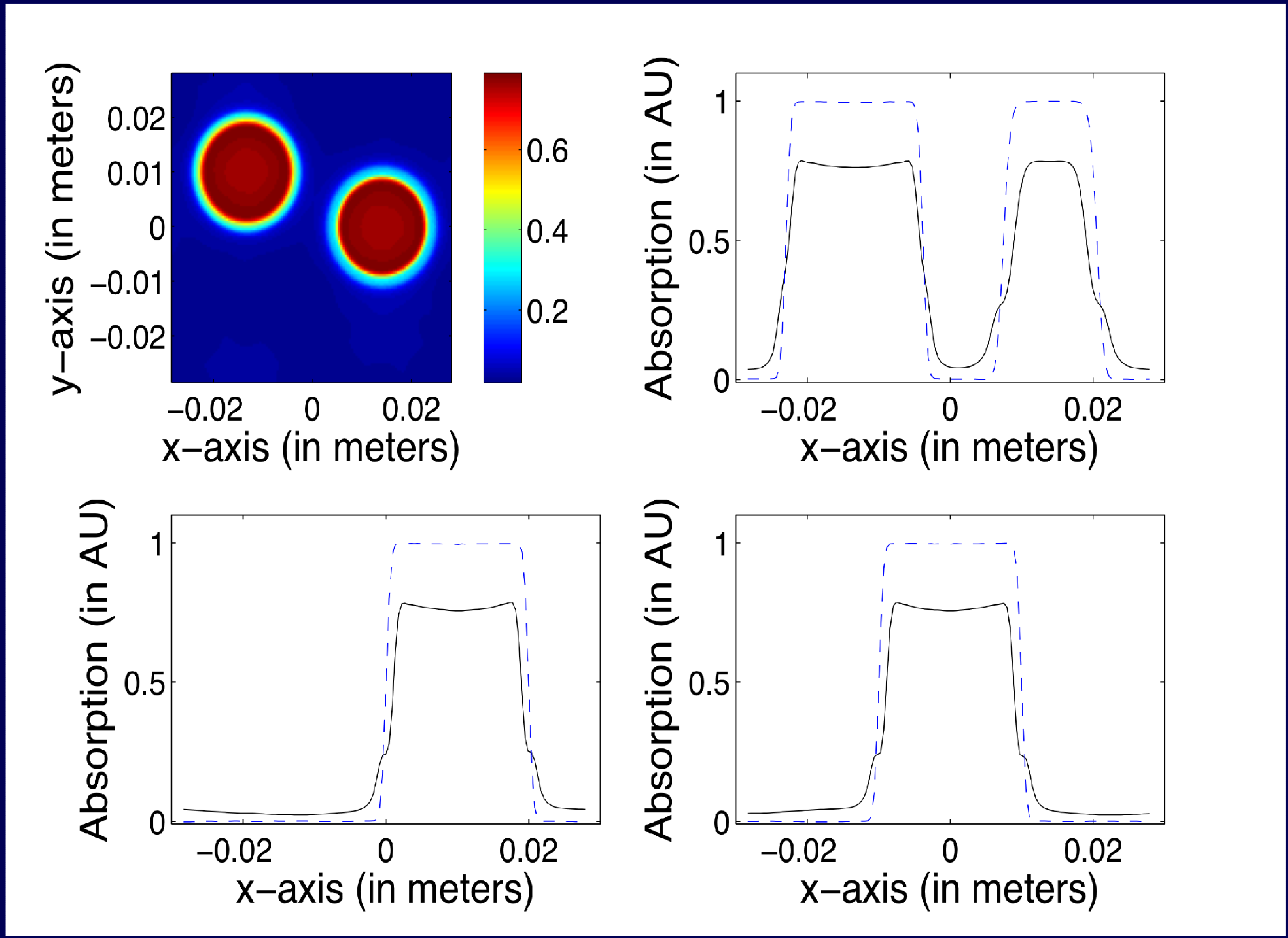

Washington University in St. Louis
School of Engineering & Applied Science

Incorporation of shear waves in PAT

- Acoustic solids support two types of propagating waves
- Longitudinal waves (also supported in fluids) and transverse waves (shear waves)

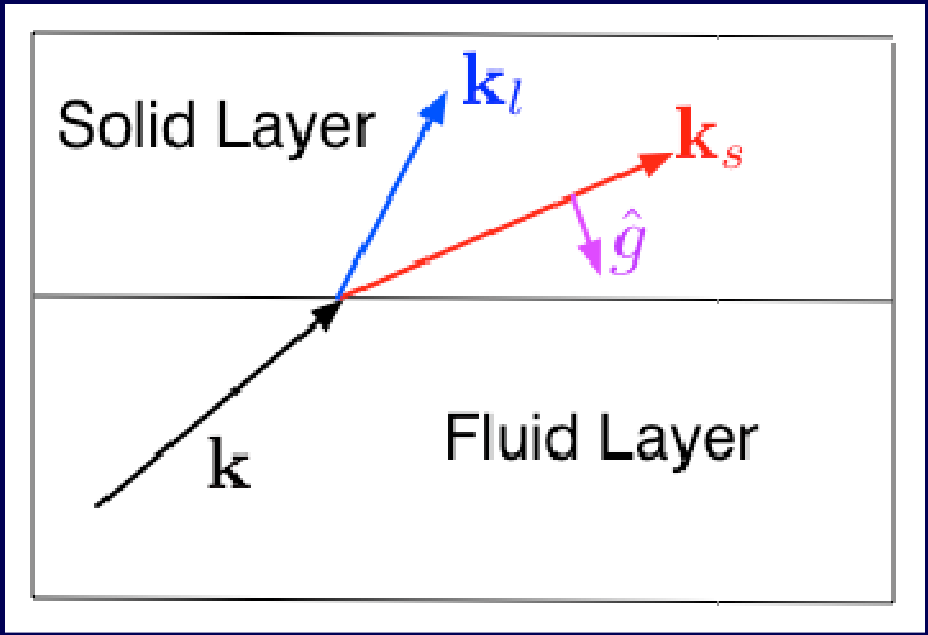

• We have extended our analysis to include shear wave physics

-- PAT reconstruction formula for layered media including elastic solids

Summary

- Incorporation of the transducer response into the imaging model facilitates accurate solution of the acoustic inverse problem.
- Use of accurate image models with iterative methods can facilitate limited data image reconstruction.
- For planar measurement geometries and layered media close-form inversion formulas are available
  - shear wave production in elastic solids
  - dispersion and attenuation

Washington University in St. Louis
School of Engineering & Applied Science

Acknowledgements

- NIH award EB010049

(Development of Thermoacoustic Tomography Brain imaging)

- NIH award EB09719

For more information contact:

Mark Anastasio

anastasio@wustl.edu

Washington University in St. Louis

School of Engineering & Applied Science